Hydrodynamic effects in three-dimensional microphase separation of block copolymers

Maurits, N. M.; Zvelindovsky, A. V. M.; Sevink, G.J.A.; van Vlimmeren, B. A. C.; Fraaije, J. G. E. M.

Published in:
Journal of Chemical Physics

DOI:
10.1063/1.476362

Publication date:
1998

Hydrodynamic effects in three-dimensional microphase separation of block copolymers: Dynamic mean-field density functional approach

N. M. Maurits, A. V. Zvelindovsky, G. J. A. Sevink, B. A. C. van Vlimmeren, and J. G. E. M. Fraaije

Citation: J. Chem. Phys. **108**, 9150 (1998); doi: 10.1063/1.476362
View online: https://doi.org/10.1063/1.476362
View Table of Contents: http://aip.scitation.org/toc/jcp/108/21
Published by the American Institute of Physics

Hydrodynamic effects in three-dimensional microphase separation of block copolymers: Dynamic mean-field density functional approach

N. M. Maurits, A. V. Zvelindovsky, G. J. A. Sevink, B. A. C. van Vlimmeren, and J. G. E. M. Fraaije
Groningen Biomolecular Sciences and Biotechnology Institute, Bioson Research Institute, University of Groningen, Department of Biophysical Chemistry, Nijenborgh 4, 9747 AG Groningen, The Netherlands

(Received 24 December 1997; accepted 25 February 1998)

The dynamic mean-field density functional method is used to describe phase separation including hydrodynamic effects in *specific* three-dimensional (3D) compressible copolymer liquids. We show that it is justified to use Darcy's approximation for the velocity field. This simple model enables us to reproduce both the increased domain growth and the faster removal of defects that are a result of hydrodynamics. We perform a simulation of a diblock copolymer melt to study the viscous effects in 3D. The free energy is shown to decrease twice as fast as in a simulation which only includes diffusion. The hydrodynamics are shown to become important only in the later stages of phase separation as is also predicted from theoretical analysis. The separation process proceeds faster because the growth of bulk domains is accelerated compared to the purely diffusive case. © *1998 American Institute of Physics.* [S0021-9606(98)51021-5]

If a complex fluid is quenched into the unstable region of its phase diagram, spinodal decomposition causes the system to spontaneously form and grow domains of different phases. This domain growth is controlled by a variety of transport mechanisms such as mass, momentum and heat transport[1]. The determination of domain growth exponents has been the object of a lot of experimental (see the references in Ref. 2) and theoretical[3] research and has led to a number of theoretical approaches to (micro-)phase separation in the presence of hydrodynamic interactions. Most numerical studies are limited to two-dimensional (2D) systems where the computational efforts are reasonable. Flow effects are incorporated in a modified Cahn–Hilliard model to study spinodal decomposition in a Hele–Shaw cell by the cell dynamical system approach in Refs. 4 and 5. In Refs. 6–8 a Langevin fluid model with conserved order parameter and current which are coupled as in the standard model H^1, is studied computationally. The same principles, using a time-dependent Ginzburg–Landau formulation, are followed in Ref. 9. In Ref. 10 the computational complexity of this approach is simplified by studying the vorticity-streaming function formulation, which can be done for incompressible 2D systems only. A different approach to modelling the hydrodynamics of phase separation in 2D is provided by the lattice Boltzmann technique[11–13] which is well suited to investigate phenomena on a hydrodynamic length and time scale, but is extremely computationally demanding in three dimensions. An extensive discussion about lattice gas and lattice Boltzmann methods in 2D and 3D can be found in Ref. 14. Another recent method to simulate hydrodynamic behavior in 2D and 3D is dissipative particle dynamics.[15] This method can also be applied to polymer liquids.[16]

It is known that other physical mechanisms become relevant in 3D,[3] which results in different domain growth. Since the early nineties, several (numerical) methods have therefore been developed to access the physical phenomena related to phase separation in 3D. In Ref. 2 a 3D Langevin fluid model which incorporates full hydrodynamic coupling is studied. In Refs. 17–19 a more simplified 3D model is described; the inertia terms in the incompressible Navier–Stokes equation are neglected giving the Stokes equation, which results in Oseen tensor hydrodynamics. These equations are integrated using the cell dynamics method. In Ref. 20 the Cahn–Hilliard theory of phase separation is extended to include hydrodynamics by use of a volumetric body force in the Stokes equation. All methods described above employ phenomenological free energies to describe the system under consideration and therefore fail to describe specific systems. In the present paper we employ the dynamic mean-field density functional method to describe phase separation, including hydrodynamic effects in *specific* 3D copolymer liquids. The relevance of our numerical experiments compared to laboratory experiments will be further improved by including hydrodynamic effects. It is known that, especially for low viscosity liquids or at later times, hydrodynamic flows enable the system to remove its topological defects. In general, the phase separation process proceeds faster (the growth of bulk domains is accelerated) in the presence of hydrodynamic modes. By applying shear[21,22] or, to some extent, by inclusion of thermal fluctuations, structural disorder can also be removed. In this paper we show that inclusion of hydrodynamic effects into the 3D dynamic mean-field density functional method in a simplified way enables us to reproduce both the increased domain growth and removal of defects.

The dynamic mean-field density functional theory[23,24] models the behavior of complex fluids by combining Gaussian mean-field statistics with a coarse-grained Ginzburg–Landau model for time evolution of conserved order parameters. In contrast to traditional phenomenological free energy expansion methods[25–27] we do not truncate the free energy at a certain level, but rather retain the full polymer path integral by a numerical procedure.[24,28,29] At present, density func-

tional theory is well established in various areas of condensed matter physics and chemical physics, from electron gas theory to the theory of liquids (see, e.g., Ref. 30). We develop a dynamic density functional theory applied to complex polymer systems.[23,24] Recently, other groups have also started to study this approach.[31,32] Although the repeated calculation of the polymer path integral is computationally very intensive, this approach allows for a description of the mesoscopic dynamics of *specific* complex liquids without constantly adjusting the parameters. Changes in the molecular properties are immediately reflected in the free energy, which enables practical application of the method. Recently, the dynamic mean-field density functional method has been successfully used to reproduce a Pluronic/water phase diagram.[33]

In the dynamic mean-field density functional approach a polymer solution is modeled as a compressible system of ideal Gaussian chain molecules. The free energy functional is given by[24,29]

$$F[\{\rho_I\}] = -kT\ln\frac{\Phi^{n_p}\Phi^{n_s}}{n_p!\,n_s!} - \sum_I \int_V U_I(\mathbf{r})\rho_I(\mathbf{r})d\mathbf{r} + \frac{1}{2}\sum_{IJ} \int_{V^2} \epsilon_{IJ}(|\mathbf{r}-\mathbf{r}'|)\rho_I(\mathbf{r})\rho_J(\mathbf{r}')d\mathbf{r}d\mathbf{r}' + \frac{\kappa_H}{2}\int_V \left(\sum_I \nu_I(\rho_I(\mathbf{r})-\rho_I^0)\right)^2 d\mathbf{r}, \tag{1}$$

where n_p (n_s) is the number of polymer (solvent) molecules, Φ is the intra-molecular partition function, I is a component index and V is the system volume. The external potentials U_I are conjugate to the density fields ρ_I via the Gaussian chain density functional. The average density is ρ_I^0 and ν_I is the bead volume. The cohesive interactions between chains have kernels $\epsilon_{IJ} \propto \epsilon_{IJ}^0 \exp[-3/(2a^2)(\mathbf{r}-\mathbf{r}')^2]$ and κ_H is the Helfand compressibility parameter.[29]

To account for hydrodynamic effects, one can employ a generalized Langevin equation of the following form:[7]

$$\frac{\partial \rho_I}{\partial t} = \sum_J \Gamma_{IJ}\frac{\delta F[\{\rho\}]}{\delta \rho_I} + V_I[\{\rho\}] + g_I^d. \tag{2}$$

The first term on the right-hand side accounts for thermal diffusion and viscous drag effects and the second term are the streaming velocities, which in our case represent simple convection terms. A general derivation is given by Farrell and Valls,[7] who calculate the streaming velocities using Poisson brackets. The noise term g_I^d is distributed according to a fluctuation–dissipation theorem. The generalized Langevin equation—Equation (2)—leads to a diffusion–convection equation for the density fields. Substituting a local coupling approximation for the kinetic coefficients[34] in Equation (2) results in

$$\frac{\partial \rho_I}{\partial t} = M_I \nabla\cdot\rho_I\nabla\mu_I - \nabla\cdot(\rho_I\mathbf{v}) + g_I^d, \tag{3}$$

where M_I is a mobility coefficient and $\mu_I \equiv \delta F/\delta\rho_I$ is the chemical potential; the noise term θ_I is distributed according to[35]

$$\langle g_I^d(\mathbf{r},t)\rangle = 0,$$

$$\langle g_I^d(\mathbf{r},t), g_J^d(\mathbf{r}',t')\rangle = -2kT\delta_{IJ}M_I\nabla\cdot\rho_I\nabla\delta(\mathbf{r}-\mathbf{r}')\delta(t-t')$$

In principle, the velocity field $\mathbf{v}$ can be obtained from the Navier–Stokes equation:[36,37]

$$\rho\left[\frac{\partial \mathbf{v}}{\partial t} + (\mathbf{v}\cdot\nabla)\mathbf{v}\right] = -\mathbf{f} + \eta\Delta\mathbf{v} + \left(\zeta + \frac{1}{3}\eta\right)\nabla\nabla\cdot\mathbf{v} \tag{4}$$

where ρ is the total density field, $\mathbf{v}$ the velocity field, $\mathbf{f}$ the external force per volume and η and ζ are viscosity coefficients. For practical purposes and to limit the computational intensity of our algorithms we approximate Equation (4). At low Reynolds numbers, the inertial term can be neglected. We neglect the acceleration, assuming that the velocity relaxation takes place more rapidly than the relaxation of concentration fluctuations. We consider systems which are slightly compressible. In this case, $(\zeta+\frac{1}{3}\eta)\nabla\nabla\cdot\mathbf{v}$ is small compared to $\eta\Delta\mathbf{v}$ in a low order approximation. The resulting Stokes equation can be solved explicitly which results in the velocity being proportional to a weighted nonlocal average of the force (Oseen tensor hydrodynamics[18]). If we further assume that this averaging is local (a delta-function Oseen tensor) we find that the local velocity is proportional to the local body force (see also Ref. 4):

$$\chi\mathbf{v}(\mathbf{r}) = \mathbf{f}(\mathbf{r}). \tag{5}$$

This is basically Darcy's law for permeable media,[36] which states that the fluid flux through a piece of porous medium is proportional to the pressure gradient applied across it. Darcy's law has already been applied to complex fluids in the cell dynamical system approach[4,5] to describe the effective local friction force. In this case, the proportionality factor χ is related to the reduced monomer mobility.[38,39] Intuitively, we can understand the application of Darcy's law in copolymer melts as follows. If a natural copolymer system is considered on a mesoscopic scale, it is highly inhomogeneous and consists of many domains which are rich in one of the components. The different domains will, in general, have different viscosities. Since the 3D mesoscale structure acts as a topological constraint to large-scale hydrodynamic flow and as hydrodynamics is more important in the lower viscosity regions, the Oseen tensor is effectively shielded on the length scale of domains. In the limit where a polymer solution can be treated as a network containing close packed (solvent) capillaries it can be shown that χ scales as η/ξ^2 where ξ is a characteristic size.[36,40] The scaling factor can be determined in the limit where each polymer chain can be treated as a sequence of blobs. In this case the Stokes friction factor can be applied to each blob and $\chi = 6\pi\eta/\xi^2$. Since the viscosity of most liquids (e.g., water, oil, glycerol) varies between 1 and 1000 cp at room temperature and the characteristic size can be estimated to be between 1 and 100 nm, χ is in the order of $10^{11}-10^{18}$ kg/ms.

Using approximation (5) for the velocity field $\mathbf{v}$ the basic features of the microscopic nonlocal hydrodynamic interactions between the polymer chains are conserved. Model (5) also correctly shows that flow effects are less dominant in

highly viscous liquids. In principle, a stochastic noise term $\mathbf{g}^v$ has to be added to the right-hand side of Eq. (5) which in this case is distributed according to

$$\langle \mathbf{g}^v(\mathbf{r},t)\rangle = 0,$$

$$\langle \mathbf{g}^v(\mathbf{r},t),\mathbf{g}^v(\mathbf{r}',t')\rangle = -2kT\chi\delta(\mathbf{r}-\mathbf{r}')\delta(t-t').$$

However, there is ample discussion about the influence of noise in numerical simulations. There is some evidence that for deep quenches, thermal noise can be neglected because in the late stages of domain growth convective effects are dominant.[17,20,10] Noise is by itself ineffective in bringing the system to global equilibrium,[13] but it facilitates reorganization of domain structure and causes domains to grow more rapidly.[2,9] Therefore, we choose to apply the diffusive noise g_I^d only. Since hydrodynamics is mainly of importance for the late stages of phase separation where the noise is less influential, it is justified to neglect the contribution of the convective noise for the moment.

The driving force per volume $\mathbf{f}$ in Eq. (5) can be obtained by a virtual work principle.[18] In a compressible system, an infinitesimal displacement $\mathbf{r}\rightarrow\mathbf{r}+\mathbf{u}(\mathbf{r})$ induces a change in the density of $\delta\rho(\mathbf{r}) = -\mathbf{u}(\mathbf{r})\cdot\nabla\rho(\mathbf{r}) - \rho(\mathbf{r})\nabla\cdot\mathbf{u}(\mathbf{r})$. Now the decrease in the free energy can be equated to the work done on the fluid body by $\mathbf{f}(\mathbf{r})$:

$$\begin{aligned}\int_V \mathbf{f}(\mathbf{r})\cdot\mathbf{u}(\mathbf{r})d\mathbf{r} &\equiv -\delta F[\{\rho\}]\\ &= -\int_V \frac{\delta F}{\delta\rho(\mathbf{r})}\delta\rho(\mathbf{r})d\mathbf{r}\\ &= \int_V \mu(\mathbf{r})\mathbf{u}(\mathbf{r})\cdot\nabla\rho(\mathbf{r})d\mathbf{r}\\ &\quad + \int_V \mu(\mathbf{r})\rho(\mathbf{r})\nabla\cdot\mathbf{u}(\mathbf{r})d\mathbf{r}\\ &= \int_V \mu(\mathbf{r})\mathbf{u}(\mathbf{r})\cdot\nabla\rho(\mathbf{r})d\mathbf{r}\\ &\quad - \int_V \nabla(\mu(\mathbf{r})\rho(\mathbf{r}))\cdot\mathbf{u}(\mathbf{r})d\mathbf{r}.\end{aligned}$$

Here we have used that $\nabla\cdot(\mu\rho\mathbf{u}) = \mu\rho\nabla\cdot\mathbf{u} + \mathbf{u}\cdot\nabla(\mu\rho)$ and $\mathbf{u}=0$ at infinity. Generalizing this derivation to multiple component systems, since $\mathbf{u}$ is arbitrary, we have that

$$\mathbf{f}(\mathbf{r}) = -\sum_I \rho_I(\mathbf{r})\nabla\mu_I(\mathbf{r}) \tag{6}$$

for compressible systems. This result shows that the local force density associated with local stresses is simply a weighted average of the thermodynamic driving forces μ_I. This is consistent with the Gibbs–Duhem equation. Hence, the resulting convection–diffusion model is given by

$$\begin{aligned}\frac{\partial\rho_I}{\partial t} &= M_I\nabla\cdot\rho_I\nabla\mu_I + \frac{1}{\chi}\nabla\cdot\rho_I\sum_J \rho_J\nabla\mu_J\\ &\quad + \frac{1}{\chi}\nabla\cdot\rho_I\mathbf{g}^v + g_I^d.\end{aligned} \tag{7}$$

Equation (7) shows that the convection basically adds (nonlinear) diffusional relaxation to the process; this effect increases with increasing inhomogeneity. Hydrodynamics clearly acts as a renormalization of diffusion.[41] For a two-component system:

$$\begin{pmatrix} M_A\nabla\cdot\rho_A\nabla & 0\\ 0 & M_B\nabla\cdot\rho_B\nabla\end{pmatrix} \rightarrow \begin{pmatrix} M_A\nabla\cdot\rho_A\nabla + \frac{1}{\chi}\nabla\cdot\rho_A^2\nabla & \frac{1}{\chi}\nabla\cdot\rho_A\rho_B\nabla\\ \frac{1}{\chi}\nabla\cdot\rho_A\rho_B\nabla & M_B\nabla\cdot\rho_B\nabla + \frac{1}{\chi}\nabla\cdot\rho_B^2\nabla\end{pmatrix}. \tag{8}$$

The additional terms are quadratic in the order parameters ρ_A and ρ_B. The renormalization therefore reflects the second order nature of the hydrodynamics. It is easy to show that the convection term further decreases the free energy in this model (neglecting the noise):

$$\begin{aligned}\frac{\partial F}{\partial t} &= \int_V \sum_I \frac{\delta F}{\delta\rho_I}\frac{\partial\rho_I}{\partial t}dV\\ &= -\int_V \sum_I \mu_I\nabla\cdot(\rho_I\mathbf{v})dV\\ &= \frac{1}{\chi}\sum_{IJ}\int_V \mu_I\nabla\cdot(\rho_I\rho_J\nabla\mu_J)dV\\ &= -\frac{1}{\chi}\sum_{IJ}\int_V \rho_I\rho_J\nabla\mu_I\cdot\nabla\mu_J dV\\ &= -\frac{1}{\chi}\int_V \left|\sum_I \rho_I\nabla\mu_I\right|^2 dV \leqslant 0.\end{aligned} \tag{9}$$

The dynamic equations (7) are closed by the expression for the free energy (1) and the Gaussian chain density functional.

In order to study viscous effects in 3D we have chosen an A_8B_8 polymer melt. The dimensionless interaction parameters are $\beta\epsilon_{AA}^0/\nu = \beta\epsilon_{BB}^0/\nu = 0.0$ and $\beta\epsilon_{AB}^0/\nu = 1.0$ where $\beta = 1/(k_BT)$. The dimensionless compressibility parameter $\beta\kappa_H\nu = 30.0$. All mobility coefficients M and bead volumes ν are identical. The dimensionless densities $\theta_I = \nu\rho_I$ are integrated numerically by a Crank–Nicolson scheme on a $32\times32\times32$ cubic grid for 2500 dimensionless time steps $\Delta\tau = \beta^{-1}Mh^{-2}\Delta t$. Here h is the grid size and Δt is the discretized time step. We have performed a simulation with only diffusion $(1/(\chi M\nu) = 0)$ and a simulation for the convection–diffusion model (Equation (7)) where the dimensionless velocity factor is $1/(\chi M\nu) = 1.62$. Here we applied the Stokes friction factor to estimate χ: $\eta = 1000$ cp which is reasonable for rather viscous liquids and the characteristic length scale $\xi = 1$ nm. All other parameters and details on the numerical integration procedure can be found in Refs. 24 and 35. As can be observed from Fig. 1 in which the order parameters $\omega \equiv (1/V)\int_V(\theta_A^2(\mathbf{r}) - \theta_{0,A}^2)d\mathbf{r}$ have been plotted, there is a crossover to a hydrodynamic regime after $\tau\approx250$. This clearly illustrates that hydrodynamics are only impor-

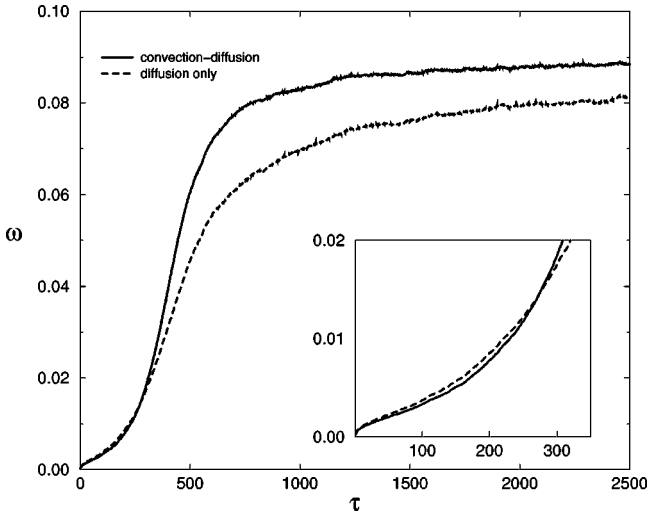

FIG. 1. Dimensionless order parameter ω as a function of dimensionless time τ.

tant during the later stages of (micro-)phase separation, which is also predicted by analytical arguments.[3]

For the simulation of the convection–diffusion model, the ordering (domain growth) proceeds faster after $\tau \approx 250$ and more defects are removed. The order parameter stabilizes at a higher value ($\omega = 0.088$) than in the simulation with only diffusion ($\omega = 0.081$) which implies that the average domain size is larger. The influence of hydrodynamic flows on the later stages of domain growth is clearly visible, but the effect is limited as we may expect in the rather viscous polymer melt. The influence of hydrodynamic flows clearly depends on the parameter χ. As we showed analytically [Equation (9)], the free energy is always lower and decreases faster (in fact almost twice as fast for this choice of χ) in the simulation which includes convective flows (Fig. 2). Figure 2 also clearly shows that the inclusion of hydrodynamic effects damps the fluctuations to a large extent.

When hydrodynamic modes are present, the frustration in the system is alleviated and the separation process proceeds faster because the growth of bulk domains is accelerated compared to the purely diffusive case.[9,13,10] In Fig. 3 we show isosurface representations of the A_8B_8 diblock copolymer melt at $\tau = 1000$ and at $\tau = 2500$ for the simulation with only diffusion and the simulation of the convection–diffusion model.

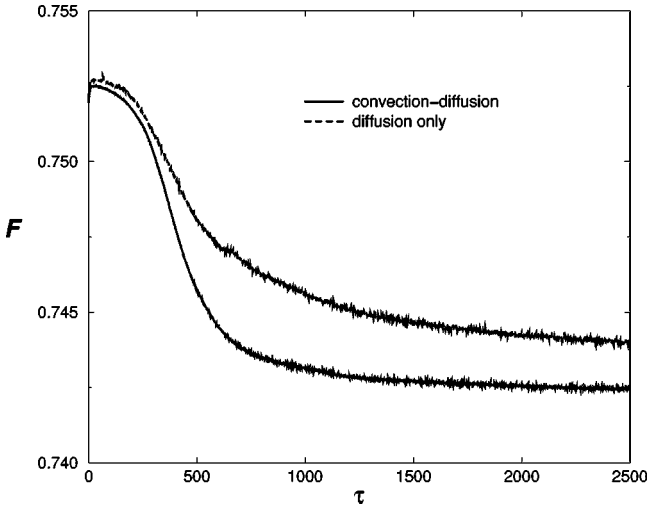

FIG. 2. Free energy F in units kT as a function of dimensionless time τ.

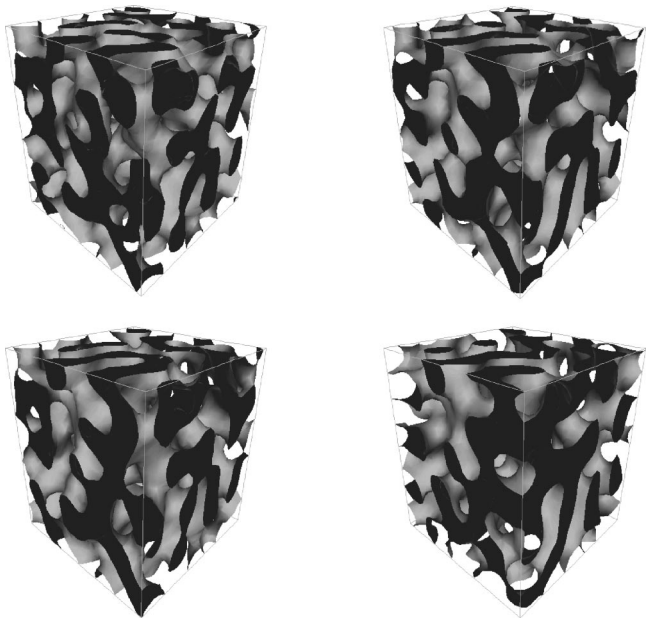

FIG. 3. Isosurface representations of the A_8B_8 diblock copolymer melt for $\theta_A = 0.5$ at $\tau = 1000$ (top) and $\tau = 2500$ (bottom) for the simulation with only diffusion (left) and the simulation of the convection–diffusion model (right).

Figure 3 also illustrates that hydrodynamic effects enhance the removal of defects and that domain growth proceeds faster if hydrodynamics is included. The morphologies at $\tau = 1000$ for the simulation of the convection–diffusion model and at $\tau = 2500$ for the simulation with only diffusion are almost the same, stressing again that the process of micro-phase separation is speeded-up considerably by hydrodynamic flow. The morphology at $\tau = 2500$ for the simulation of the convection–diffusion model is clearly further developed towards a lamellar morphology.

The influence of hydrodynamics on phase separation can also be observed from the time dependent structure factor, which was calculated as the angle average of $|\theta_A(\mathbf{k})|$, where $\theta_A(\mathbf{k})$ is the Fourier transform of the density $\theta_A(\mathbf{r})$. Notice that high frequencies are undersampled because of the limited box size. The maximum frequency in the box is $h^{-1}\sqrt{3}/2$. In Fig. 4 the structure factor is plotted at different time levels for the simulation of the convection–diffusion model of the A_8B_8 diblock copolymer melt. We clearly observe the shift of the peak to lower frequencies as time proceeds, which corresponds to growth of the domains. The higher order Bragg peaks that may be expected from a lamellar morphology have not yet developed in this short simulation, although a slight shoulder can already be observed for $\tau = 2500$. Figure 5, in which structure factors of both 3D simulations are plotted for comparison, also demonstrates that the domain growth is faster if hydrodynamic effects are added to the pure diffusion model.

In these numerical simulations we have shown that a very simple model based on Darcy's law for permeable me-

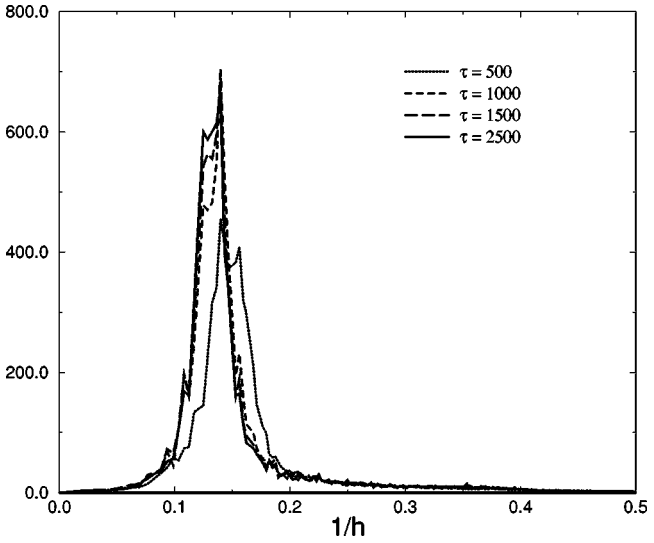

FIG. 4. Structure factors in arbitrary units for the A_8B_8 diblock copolymer melt; simulation of the convection–diffusion model. Displayed are the structure factors at $\tau=500$, $\tau=1000$, $\tau=1500$ and $\tau=2500$. The frequency is in units $1/h$.

dia can account for the physical effects that are caused by hydrodynamics. The domain growth is increased and defects are removed faster. We realize that much more sophisticated models could be used for the 3D velocity field.[2] However, since we are primarily interested in predicting phases for *specific* complex liquids, a simple model already gives a good average picture of the influence of viscous effects. The precise position of domain boundaries is of less interest for our purposes. The most rigorous approximation in our model for the velocity field is to assume that it is proportional to the local force density. The local approximation for the viscous friction force may be justified because in concentrated phase-separated systems, the domains shield the flow to a large extent. Moreover, the 3D mesoscale structure itself acts as a topological constraint to large-scale hydrodynamic flow (see also Ref. 4). However, a full description of hydrodynamics should take a concentration-dependent viscosity into account.[41] This will complicate the description of the microphase separating melt to a limited extent, and will be done in the near future. A second improvement to our description would be to take the nonlocal character of hydrodynamic flow explicitly into account. Notice that we already account for nonlocality in the intramolecular model by the chain connectivity and in the mean-field contribution to the free energy. We have also shown that it is possible to account for nonlocality in the kinetic model[34] and we intend to study hydrodynamic effects in this regime as well. Another important nonlocal effect in complex liquids is of (visco)elastic origin. In order to be able to study rheological properties of these materials we are currently investigating the incorporation of memory effects in our model.

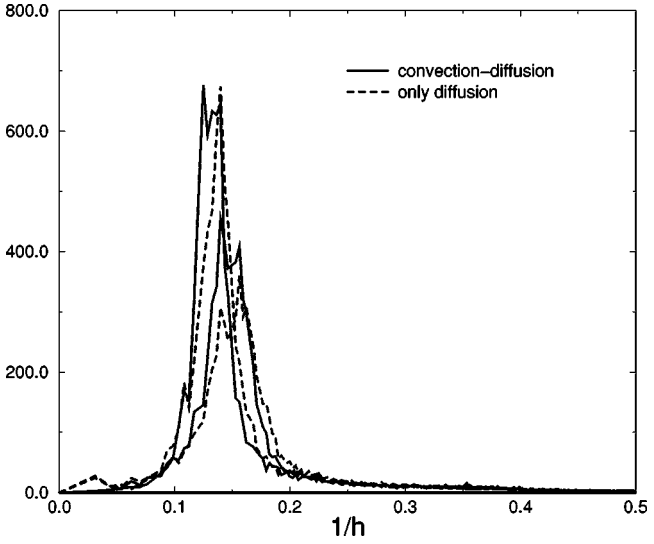

FIG. 5. Structure factors in arbitrary units for the A_8B_8 diblock copolymer melt; simulations of the convection–diffusion model and of the model with only diffusion. Displayed for both simulations are the structure factors at $\tau=500$ and $\tau=2500$. The frequency is in units $1/h$.

[1] P. C. Hohenberg and B. I. Halperin, Rev. Mod. Phys. **49**, 435 (1977).
[2] O. T. Valls and J. E. Farrell, Phys. Rev. E **47**, R36 (1993).
[3] E. D. Siggia, Phys. Rev. A **20**, 595 (1979).
[4] M. Bahiana and Y. Oono, Phys. Rev. A **41**, 6763 (1990).
[5] A. Shinozaki and Y. Oono, Phys. Rev. A **45**, 2161 (1992).
[6] O. T. Valls and G. F. Mazenko, Phys. Rev. B **38**, 11643 (1988).
[7] J. E. Farrell and O. T. Valls, Phys. Rev. B **40**, 7027 (1989).
[8] J. E. Farrell and O. T. Valls, Phys. Rev. B **43**, 630 (1991).
[9] G. Pätzold and K. Dawson, Phys. Rev. E **52**, 6908 (1995).
[10] H. Chen and A. Chakrabarti, Phys. Rev. E **55**, 5680 (1997).
[11] M. R. Swift, W. R. Osborn, and J. M. Yeomans, Phys. Rev. Lett. **75**, 830 (1995).
[12] W. Osborn *et al.*, Phys. Rev. Lett. **75**, 4031 (1995).
[13] G. Gonnella, E. Orlandini, and J. M. Yeomans, Phys. Rev. Lett. **78**, 1695 (1997).
[14] D. H. Rothman and S. Zaleski, Rev. Mod. Phys. **66**, 1417 (1994).
[15] P. J. Hoogerbrugge and J. M. V. A. Koelman, Europhys. Lett. **19**, 155 (1992).
[16] R. D. Groot and P. B. Warren, J. Chem. Phys. **107**, 4423 (1997).
[17] T. Koga and K. Kawasaki, Phys. Rev. A **44**, R817 (1991).
[18] K. Kawasaki, T. Koga, and T Kawakatsu, Mater. Res. Soc. Symp. Proc. **237**, 87 (1992).
[19] A. Shinozaki and Y. Oono, Phys. Rev. E **48**, 2622 (1993).
[20] N. Vasishtha and E. B. Nauman, Chem. Eng. Commun. **129**, 29 (1994).
[21] A. Onuki, J. Phys.: Condens. Matter **9**, 6119 (1997).
[22] A. V. Zvelindovsky *et al.*, Phys. Rev. E (to be published).
[23] J. G. E. M. Fraaije, J. Chem. Phys. **99**, 9202 (1993).
[24] J. G. E. M. Fraaije *et al.*, J. Chem. Phys. **106**, 4260 (1997).
[25] J. W. Cahn and J. E. Hilliard, J. Chem. Phys. **28**, 258 (1958).
[26] Y. Oono and S. Puri, Phys. Rev. Lett. **58**, 836 (1987).
[27] P. G. de Gennes, J. Chem. Phys. **72**, 4756 (1980).
[28] N. M. Maurits, P. Altevogt, O. A. Evers, and J. G. E. M. Fraaije, Comput. Polym. Sci. **6**, 1 (1996).
[29] N. M. Maurits, B. A. C. van Vlimmeren, and J. G. E. M. Fraaije, Phys. Rev. E **56**, 816 (1997).
[30] *Recent Developments and Applications of Modern Density Functional Theory*, edited by J. Seminario (Elsevier, Amsterdam, 1996).
[31] R. Hasegawa and M. Doi, Macromolecules **30**, 3086 (1997).
[32] T. Kawakatsu, Phys. Rev. E **56**, 3240 (1997).
[33] B. A. C. van Vlimmeren *et al.* (unpublished).
[34] N. M. Maurits and J. G. E. M. Fraaije, J. Chem. Phys. **107**, 5879 (1997).
[35] B. A. C. van Vlimmeren and J. G. E. M. Fraaije, Comput. Phys. Commun. **99**, 21 (1996).
[36] G. K. Batchelor, *An Introduction to Fluid Dynamics* (Cambridge University Press, Cambridge, 1967).
[37] L. D. Landau and E. M. Lifshitz, *Fluid Mechanics*, 2nd ed. (Pergamon, Oxford, 1987).
[38] P.-G. de Gennes, Macromolecules **9**, 594 (1976).
[39] A. V. Zvelindovsky and D. Bedeaux, Physica A **222**, 87 (1995).
[40] J. Harden, H. Pleiner, and P. Pincus, J. Chem. Phys. **94**, 5208 (1991).
[41] G. H. Fredrickson, J. Rheol. **38**, 1045 (1994).